Submitted: 08 March, 2025 Accepted: 30 May, 2025 Published: 30 July, 2025 DOI:10.22514/jomh.2025.102

ORIGINAL RESEARCH

JOMH Journal of Men's Health

The toxicity and mechanisms of pyrotinib on male reproductive system

Xiao Hu[1,*,†], Zhongjian Pan[1,†], Jie Yang[2], Peng Zheng[1], Jian Tan[1], Zhipeng Xu[1], Huaming Tang[1], Jianpeng Hu[1]

[1]Department of Urology, the First People's Hospital of Zhenjiang, 212000 Zhenjiang, Jiangsu, China
[2]School of Medicine, Jiangsu University, 212000 Zhenjiang, Jiangsu, China

***Correspondence**
liuliping@ujs.edu.cn
(Xiao Hu)

[†] These authors contributed equally.

Abstract

Background: While Pyrotinib is effective in treating human epidermal growth factor receptor 2 (HER2)-positive breast cancer, its impact on male reproductive health remains unclear. This study investigates the potential reproductive toxicity and underlying mechanisms of Pyrotinib in male Leydig cells, key regulators of testosterone production. **Methods**: Leydig cells were treated with Pyrotinib, with 0.1‰ dimethyl sulfoxide (DMSO)-treated cells serving as the control group, to evaluate its effects on cell viability, apoptosis, cell cycle progression and signaling pathways. Clonogenic assays, flow cytometry, Western blotting and transcriptome sequencing were employed. **Results**: Pyrotinib treatment for 24 hours significantly reduced cell viability and colony formation while increasing apoptosis. Flow cytometry revealed G1 phase arrest in 67.2% of cells after Pyrotinib exposure. Western blot analysis showed transient activation of Ak strain transforming (AKT) and extracellular signal-regulated kinase (ERK) at 2 hours, followed by marked inhibition at 24–48 hours. Transcriptomic analysis identified 197 downregulated genes enriched in chromatin organization and mitotic processes, particularly cell cycle regulation. **Conclusions**: Pyrotinib impairs Leydig cell proliferation through G1 arrest and inhibition of the phosphoinositide 3-kinase (PI3K)/AKT and mitogen-activated protein kinase (MAPK)/ERK pathways, along with downregulation of cell cycle-related genes. These findings highlight the need for further evaluation of Pyrotinib's reproductive safety in male patients.

Keywords

Pyrotinib; Toxicity; Male; Leydig cells; Proliferation

1. Introduction

Targeted therapy against human epidermal growth factor receptor 2 (HER2) has become the cornerstone of treatment for both early-stage and metastatic HER2-positive breast cancer. The use of anti-HER2 monoclonal antibodies-particularly trastuzumab and pertuzumab-constitutes the standard therapeutic approach in the neoadjuvant and adjuvant settings, as well as in first-line treatment for patients with metastatic HER2-positive disease [1]. In the second-line setting, novel antibody-drug conjugates such as trastuzumab deruxtecan and trastuzumab emtansine have further expanded therapeutic options for these patients [2]. Pyrotinib, an irreversible pan-erythroblastic oncogene B (ErbB) receptor tyrosine kinase inhibitor [3], has demonstrated promising efficacy in HER2-positive breast cancer, owing to its distinctive molecular structure and pharmacodynamic properties [4–6]. However, current clinical investigations on Pyrotinib have been predominantly conducted in female cohorts, resulting in a paucity of data on its safety and efficacy in male patients.

In recent years, Pyrotinib has also been increasingly employed in the treatment of non-small cell lung cancer [7] and gastric cancer [8], thereby contributing to a growing number of male recipients of this agent. Despite this trend, limited attention has been given to the potential adverse effects of Pyrotinib on the male reproductive system, and mechanistic insights remain largely unexplored. Therefore, the present study aims to evaluate the potential reproductive toxicity of Pyrotinib in male subjects and to investigate the underlying molecular mechanisms. This work seeks to provide a more comprehensive assessment of the safety profile of Pyrotinib, thereby informing its rational clinical application in male patients.

2. Materials and methods

2.1 Cell culture of TM3 cell line

The mouse Leydig cell line TM3 was obtained from Shanghai Yuchi Biotech Co., Ltd. (SC0443) and authenticated via short tandem repeat (STR) profiling to confirm species origin. Cells were maintained in Dulbecco's Modified Eagle Medium (DMEM, Gibco, C11995500BT, Suzhou, China) sup-

plemented with 10% fetal bovine serum (FBS, Lonsera, S711-001S, Montevideo, Uruguay) and 1% penicillin-streptomycin solution (Servicebio, G4003, Wuhan, China). Cultures were incubated at 37 °C in a humidified atmosphere containing 5% CO_2, and the culture medium was refreshed every 2–3 days. Upon reaching approximately 80% confluence, cells were detached using trypsin (Beyotime) and subcultured at a 1:3 ratio. For experimental treatments, TM3 cells were exposed to various concentrations of Pyrotinib, with control cells receiving 0.1‰ dimethyl sulfoxide (DMSO) as the vehicle control. Detailed protocols for drug administration, sample collection, and downstream analyses are described in the corresponding sections.

2.2 Preparation of Pyrotinib solution

Pyrotinib, provided as an active pharmaceutical ingredient by Jiangsu Hengrui Medicine Co., Ltd. (H20180012, Lianyungang, Jiangsu, China), was initially dissolved in dimethyl sulfoxide (DMSO) to prepare a 0.1 M stock solution. The stock solution was aliquoted and stored appropriately to prevent degradation. Prior to use, the stock was diluted with TM3 culture medium to the required working concentrations for experimental treatments, ensuring the final DMSO concentration in all treatment groups did not exceed 0.1‰.

2.3 Clonogenic assay

TM3 cells were cultured until they reached 80–90% confluence and then subjected to different treatments. Cells in the experimental group were treated with 100 nM pyrotinib, while those in the control group received an equivalent volume of 0.1‰ DMSO. After 24 hours of treatment, cells were trypsinized, counted and seeded into 6-well plates at a density of 500 cells per well. The cells were then cultured under standard conditions for 14 days, with medium changed every 2–3 days. At the end of the incubation period, colonies were fixed with 4% paraformaldehyde for 10 minutes and stained with 0.5% crystal violet for 20 minutes. Colony formation was subsequently visualized and assessed under a microscope.

2.4 Cell viability assay

TM3 cells in the logarithmic growth phase were trypsinized, counted and seeded into 96-well plates at a density of 3000 cells per well. Following 24 hours of incubation to allow for cell attachment, the cells were treated with Pyrotinib at six different concentrations: 0.1 nM, 1 nM, 10 nM, 100 nM, 1000 nM and 10,000 nM. Each concentration group included three replicate wells. After an additional 24-hour exposure period, cell viability was assessed using the Cell Counting Kit-8 (CCK-8, Yisheng Biotech, 40203ES76, Shanghai, China), following the manufacturer's protocol. The CCK-8 reagent was added to each well and incubated for 1 hour at 37 °C. Absorbance was measured at 450 nm using a microplate reader. The data were used to construct a dose—response curve for Pyrotinib-induced cytotoxicity.

2.5 Cell cycle analysis

TM3 cells in the logarithmic growth phase were harvested, counted, and seeded into 6-well plates at a density of 5×10^5 cells per well. After 24 hours of incubation, cells in the experimental group were treated with 100 nM Pyrotinib, while control cells received 0.1‰ DMSO. Following a 48-hour treatment period, cells were collected and fixed in 75% ethanol at −20 °C for at least 24 hours. Cell cycle staining was performed according to the manufacturer's instructions using a commercial cell cycle analysis kit (Lianke Biotechnology, CCS012, Hangzhou, China). Data acquisition was carried out on a CytoFLEX flow cytometer (Cytoflex LX, Beckman Coulter, Brea, CA, USA), and cell cycle distribution was analyzed accordingly.

2.6 Western-blot assay

TM3 cells in the logarithmic growth phase were seeded into 6-well plates at a density of 2×10^5 cells per well. After 24 hours, cells were treated with Pyrotinib at concentrations of 0 nM, 50 nM and 100 nM. Total protein was extracted at 2, 24 and 48 hours post-treatment using RIPA lysis buffer (Beyotime, P0013B, Shanghai, China), and protein concentrations were determined using a bicinchoninic acid (BCA) assay kit (Beyotime, P0010S, Shanghai, China). Equal amounts of protein were separated on 10% sodium dodecyl sulphate (SDS)—polyacrylamide gels (1.5 mm, 15-well; Epizyme) and transferred onto polyvinylidene fluoride (PVDF) membranes (Millipore). Membranes were blocked with QuickBlock™ blocking buffer (Beyotime, P0252, Shanghai, China) and incubated with specific primary antibodies (see Table 1 for details). Detection was performed using appropriate secondary antibodies and visualized with the Bio-Rad Gel Imaging System.

2.7 Transcriptome sequencing

TM3 cells in the logarithmic growth phase were dissociated and counted, then seeded into 6-well plates at a density of 500,000 cells per well. The treatment group received 100 nM Pyrotinib, while the control group was treated with 0.1‰ DMSO, with three replicates for each group. After 48 hours of treatment, RNA was extracted using TRIzol reagent (Takara, 9108, Shiga, Japan) and sent to Beijing Novogene Co., Ltd. for transcriptome sequencing. RNA sequencing was performed on the Illumina Novaseq platform, generating approximately 150 bp paired-end reads per sample. RNA quality was assessed using the Agilent 2100 Bioanalyzer (Agilent 2100 Bioanalyzer, Agilent Technologies, Santa Clara, CA, USA) with the RNA Nano 6000 Assay Kit (5067-1511, Agilent, CA, USA). Total RNA was utilized to construct libraries through poly-A selection, followed by fragmentation, cDNA synthesis with random hexamer primers, and adaptor ligation according to the manufacturer's protocols (Agilent, Santa Clara, CA). The libraries were quantified via quantitative polymerase chain reaction (qPCR) with a KAPA Library Quantification Kit (Kapa Biosystems, KK4824, Woburn, MA, USA), and clustering was conducted on an Illumina cBot system using the TruSeq PE Cluster Kit v3-cBot-HS (PE-401-3001, San Diego, CA, USA).

TABLE 1. Antibody information used in Western blot assay.

Antibody	Company	Catalog	Dilution ratio
GAPDH	Proteintech	60004-1-Ig	1:50,000
ERK1/2	Proteintech	11257-1-AP	1:5000
Phospho-ERK1/2 (Thr202/Tyr204)	Proteintech	28733-1-AP	1:2000
AKT	Proteintech	60203-2-Ig	1:10,000
Phospho-AKT (Ser473)	Proteintech	66444-1-Ig	1:10,000
Phospho-p70 (S6K) (Thr389)	Proteintech	28735-1-AP	1:10,000

GAPDH: glyceraldehyde-3-phosphate dehydrogenase; ERK: extracellular signal-regulated kinase; AKT: Ak strain transforming.

2.8 Bioinformatic analyses

Data preprocessing was performed on the raw fastq files using fastp (v0.20.0, HaploX Biotechnology, Shenzhen, China) [9] to remove low-quality reads, reads with poly-N and adapter sequences, resulting in high-quality reads (Q20, Q30). Clean reads were aligned to the reference genome using Hisat2 (v2.0.5, Center for Computational Biology, Johns Hopkins University, Baltimore, MD, USA) [10], with gene annotations in Gene transfer format (GTF) format. Hisat2 was chosen for its ability to handle splice junctions, allowing for high-quality alignments. Reads with mapping quality of less than 30 were filtered out.

For gene expression quantification, the featureCounts tool (v1.5.0-p3, Walter and Eliza Hall Institute of Medical Research, Melbourne, VIC, Australia) [11] was used to count the reads mapped to each gene, and the FPKM (Fragments Per Kilobase of transcript per Million mapped reads) method was applied to normalize gene expression levels across samples.

Principal component analysis was performed using the FactoMineR package (v2.11, Agrocampus Ouest, Rennes, France) [12] and visualized with the factoextra package (v1.0.7, Marseille, France) to explore the overall structure of the data and visualize sample clustering. Differential expression analysis was conducted between the two groups, Pyrotinib (Py) and normal control (NC), each with three biological replicates. The DESeq2 package (v1.20.0, European Molecular Biology Laboratory, Heidelberg, BW, Germany) [13] in R was used to identify significantly differentially expressed genes, with significance defined by an adjusted *p*-value (*p*adj) $\leq$ 0.05 and an absolute Log2 fold change (|Log2 (FoldChange)| $\geq$1). Gene Ontology (GO) [14] and Kyoto Encyclopedia of Genes and Genomes (KEGG) [15] enrichment analyses were carried out using the clusterProfiler (v3.10.0, Southern Medical University, Guangzhou, China) [16], applying a corrected *p*adj $\leq$ 0.05 to determine significantly enriched terms and pathways.

All downstream analyses, including differential expression, visualization and enrichment analyses, were conducted in R (v3.5.0, R Core Team, R Foundation for Statistical Computing, Vienna, Austria).

3. Results

3.1 Pyrotinib inhibited the proliferation of TM3 cells

To evaluate the effects of Pyrotinib on the male reproductive system, TM3 mouse Leydig cells were employed as an *in vitro* model. Following 24 hours of treatment, a significant increase in apoptosis was observed in the Pyrotinib-treated group compared to the control group, as determined by flow cytometry (Fig. 1A). Clonogenic assays further demonstrated a marked decrease in colony-forming ability upon Pyrotinib exposure (Fig. 1B). A dose-dependent reduction in cell viability was also noted, with an estimated half-maximal inhibitory concentration (IC_{50}) of approximately 95.74 nM (Fig. 1C). Cell cycle analysis revealed that Pyrotinib treatment led to cell cycle arrest at the G1 phase, with 67.2% of cells in the treated group remaining in G1 compared to 58.3% in the control group (Fig. 1D,E). Collectively, these findings indicate that Pyrotinib significantly impairs the proliferative capacity and viability of TM3 cells, primarily by inducing apoptosis and arresting cell cycle progression at the G1 phase, thereby inhibiting entry into the S phase.

3.2 Pyrotinib modulates PI3K/AKT and MAPK/ERK signaling pathways in TM3 cells

To investigate the molecular mechanisms underlying the Pyrotinib-induced reduction in proliferation and viability of TM3 cells, Western blot analysis was performed. This examined the expression levels of key signaling proteins, including AKT, ERK, phosphorylated AKT (p-AKT), phosphorylated ERK (p-ERK) and phosphorylated S6 kinase (p-S6K). As shown in Fig. 2A,B (and **Supplementary Fig. 1**), short-term treatment with Pyrotinib (2 hours) led to a transient increase in the phosphorylation levels of these proteins. However, prolonged exposure to Pyrotinib (24 to 48 hours) resulted in a marked decrease in the phosphorylation levels of proteins involved in both the PI3K/AKT and MAPK/ERK signaling pathways. These results suggest that Pyrotinib may initially activate, but subsequently suppress, key proliferative and survival pathways in TM3 cells, thereby contributing to its inhibitory effects on cell growth and viability.

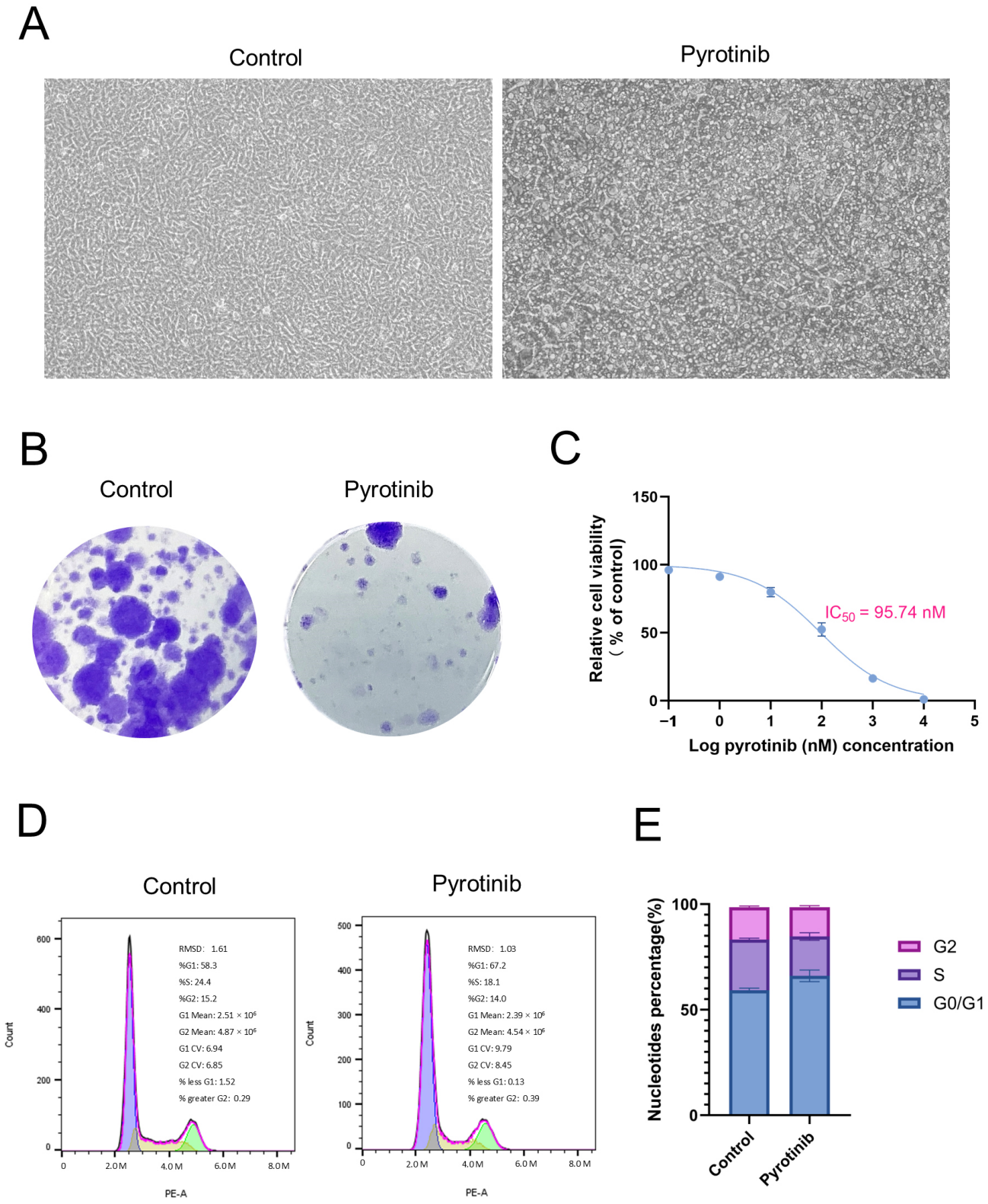

FIGURE 1. Effects of Pyrotinib on TM3 cell proliferation and cell cycle progression. (A) Pyrotinib treatment (100 nM, 24 h) significantly increased apoptosis in TM3 cells compared to the control group, as shown by representative images. Scale bar: 100 μm. (B) Colony formation assay showing a marked reduction in the number of colonies after 24 hours of Pyrotinib treatment, visualized by crystal violet staining. (C) Cell viability decreased in a dose-dependent manner with increasing concentrations of Pyrotinib; IC_{50} was approximately 95.74 nM (n = 6). (D) Flow cytometry analysis revealed that 67.2% of TM3 cells in the Pyrotinib-treated group were arrested in the G1 phase, compared to 58.3% in the control group (n = 3). (E) Quantitative comparison of cell cycle distribution between the Pyrotinib-treated and control groups (n = 3). Data are presented as mean ± standard deviation. Abbreviations: RMSD: root mean square deviation; IC_{50}: half maximal inhibitory concentration; G0: Gap 0; G1: Gap 1; G2: Gap 2; S: Synthesis; CV: coefficient of variation.

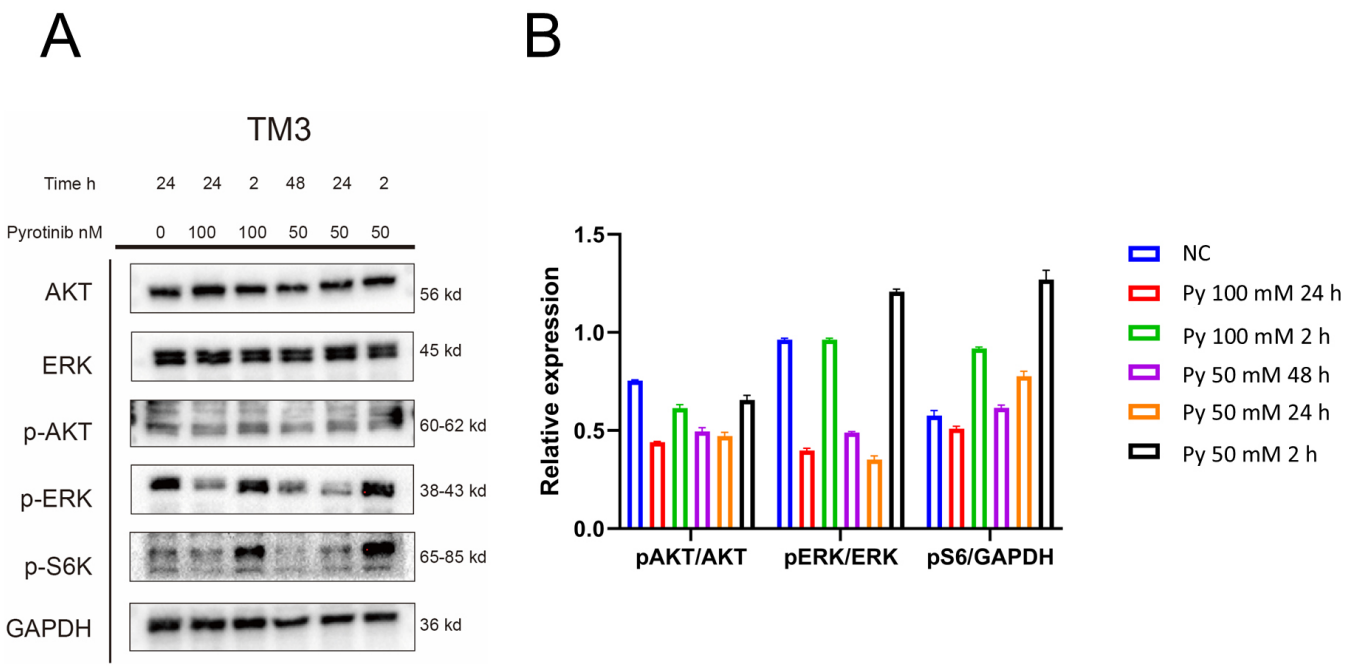

FIGURE 2. Effects of Pyrotinib on PI3K/AKT and MAPK/ERK Signaling Pathways in TM3 Cells. (A) Western blot analysis showing the expression levels of total and phosphorylated AKT, ERK and S6K following treatment with different concentrations of Pyrotinib. A transient increase in phosphorylated protein levels was observed at early time points. (B) Quantitative analysis of phosphorylated protein expression (p-AKT, p-ERK and p-S6K) at various time points, illustrating a significant reduction after 24 and 48 hours of Pyrotinib exposure. Data are presented as mean ± standard deviation (n = 3). Abbreviations: AKT: Ak strain transforming; ERK: extracellular signal-regulated kinase; p-AKT: phosphorylated AKT; p-ERK: phosphorylated ERK; p-S6K: phosphorylated S6 kinase; GAPDH: glyceraldehyde-3-phosphate dehydrogenase; NC: normal control; Py: Pyrotinib-treated group.

3.3 Transcriptomic analysis reveals molecular mechanisms underlying Pyrotinib treatment

To elucidate the molecular mechanisms mediating the effects of Pyrotinib on TM3 cells, transcriptome sequencing was conducted on samples collected prior to treatment and at 48 hours post-treatment. Principal component analysis (PCA) demonstrated clear sample clustering, with confidence ellipses encompassing all replicates within one standard deviation of the mean (Fig. 3A). Differential gene expression analysis, visualized via a volcano plot, identified 170 significantly upregulated and 197 downregulated genes following Pyrotinib exposure (Fig. 3B). Gene Ontology (GO) enrichment analysis revealed that the downregulated genes were predominantly associated with biological processes related to chromatin dynamics and mitosis, including mitotic spindle assembly, mitotic sister chromatid segregation and regulation of chromosome segregation (Fig. 3C). KEGG pathway analysis further indicated significant enrichment of these genes in the cell cycle pathway (Fig. 3D). Collectively, these data suggest that Pyrotinib exerts its antiproliferative effects in TM3 cells, at least in part, through the downregulation of key genes involved in cell cycle progression and mitotic processes.

4. Discussion

Women undergoing treatment with Pyrotinib are recommended to use effective contraception throughout the duration of therapy and for at least 8 weeks after the treatment has ended. However, due to the limited scope of its current clinical indications, studies evaluating the adverse effects of Pyrotinib in male subjects remain scarce [17–19], and none have specifically addressed its potential impact on male reproductive function. Notably, preclinical toxicity studies have reported that Pyrotinib can induce mild degeneration of the seminiferous tubules and epididymal ducts in dogs, along with histopathological features consistent with epididymal oligospermia [5].

Leydig cells, located in the interstitial compartment of the testes, are essential for androgen synthesis and male reproductive development. During fetal development, testosterone produced by Leydig cells is critical for the formation of the male reproductive tract and external genitalia, as well as for the descent of the testes. In puberty and adulthood, Leydig cell-derived testosterone is indispensable for the initiation and maintenance of spermatogenesis, maturation of reproductive organs and preservation of male fertility [20]. In this study, we investigated the effects of Pyrotinib on TM3 mouse Leydig cells to assess its potential reproductive toxicity. Our results demonstrated that Pyrotinib significantly inhibited cell proliferation and viability, while simultaneously

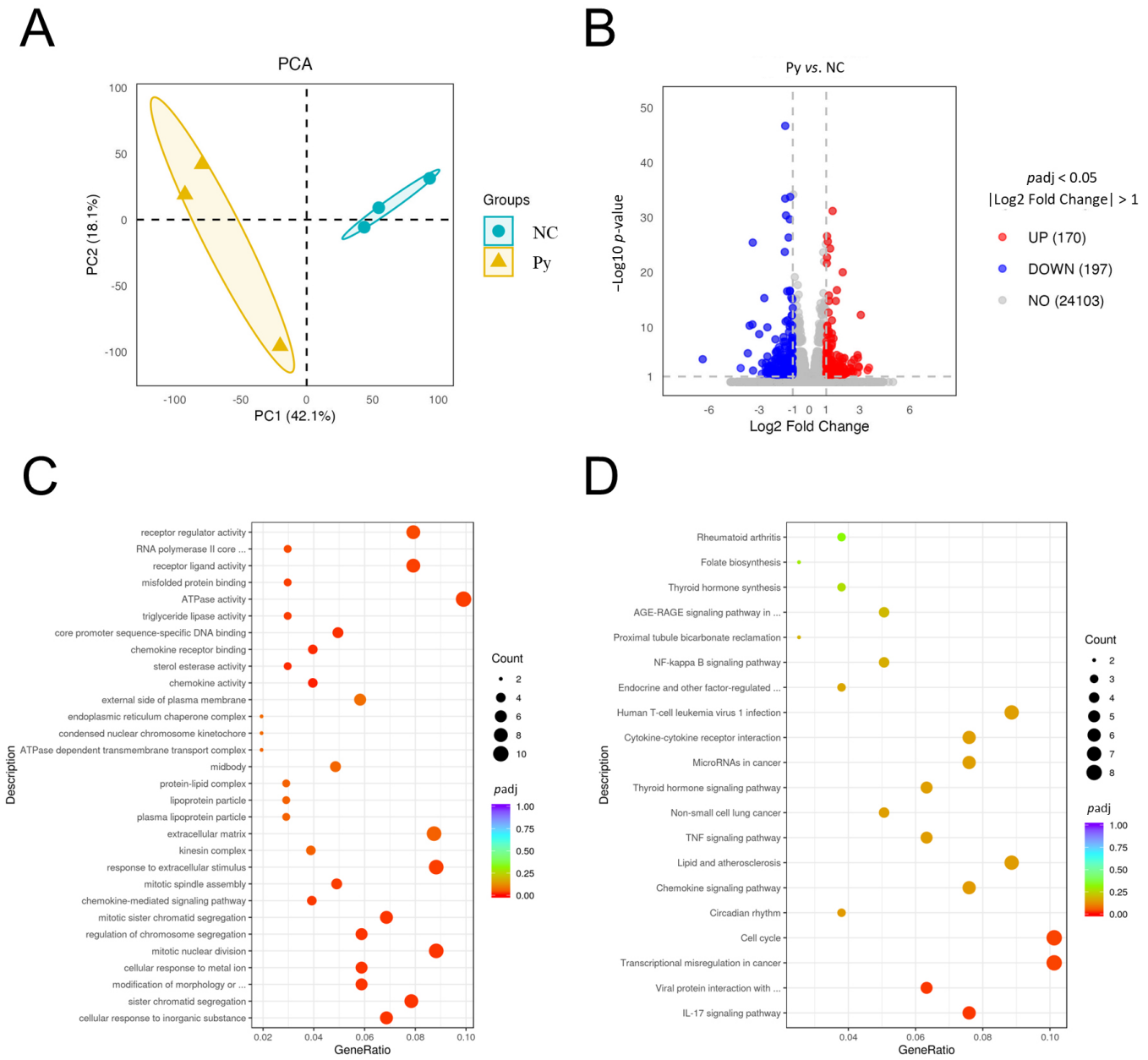

FIGURE 3. Transcriptomic and enrichment analyses following Pyrotinib treatment in TM3 cells. (A) Principal component analysis (PCA) plot illustrating the distribution of samples based on the first two principal components. Each dot represents a sample, colored by group: NC (normal control, teal) and Py (Pyrotinib-treated, yellow). (B) Volcano plot displaying differentially expressed genes between Py and NC groups. Significantly downregulated genes are shown in blue, and upregulated genes in red (adjusted $p < 0.05$, ($|\text{Log2 (FoldChange)}| \geq 1$). (C) Gene Ontology (GO) enrichment analysis of downregulated genes, showing significantly enriched biological process terms. Dot size indicates the number of genes annotated to each term, while color intensity reflects the statistical significance (adjusted p value). (D) Kyoto Encyclopedia of Genes and Genomes (KEGG) pathway enrichment analysis of downregulated genes. Enriched pathways are presented similarly to GO terms with respect to dot size and significance. Abbreviations: PC1: the first principal components; PC2: the second principal components.

inducing apoptosis. Marked apoptotic activity was observed within 24 hours of treatment, accompanied by a substantial decrease in colony-forming ability, suggesting a suppression of proliferative capacity linked to compromised cell survival. Moreover, Pyrotinib exerted a dose-dependent cytotoxic effect, with increasing concentrations resulting in progressively reduced cell viability. These findings are consistent with its known antitumor activity [21] and may offer preliminary insights into concentration-dependent thresholds relevant to both therapeutic efficacy and potential off-target reproductive toxicity.

Cell cycle analysis revealed a marked increase in the proportion of cells in the G1 phase following Pyrotinib treatment, suggesting that the drug interferes with cell cycle progression and consequently disrupts normal cellular replication. This observation aligns with findings from previous studies, further

supporting the antiproliferative role of Pyrotinib [21]. At the signaling level, Western blot analysis demonstrated that Pyrotinib significantly attenuates the activity of the PI3K/AKT and MAPK/ERK pathways. Interestingly, a transient increase in phosphorylation levels of key pathway components was observed after 2 hours of treatment, indicating an initial activation phase. However, with prolonged exposure (24–48 hours), a pronounced decrease in phosphorylation was detected, suggesting the involvement of a feedback inhibition mechanism. Transcriptomic analyses further revealed downregulation of genes involved in mitosis and cell cycle regulation, which likely contributes to the observed reduction in proliferative capacity. Both the MAPK and PI3K/AKT/mechanistic target of rapamycin (mTOR) signaling cascades are known to play pivotal roles in the pathogenesis of HER2-positive cancers. The MAPK pathway governs critical cellular functions such as proliferation, adhesion and invasion, and is closely linked to tumor aggressiveness [22]. Similarly, the PI3K/AKT/mTOR pathway is essential for tumor cell growth, survival and metastasis, and its inhibition has been associated with increased apoptosis and reduced metastatic potential [23, 24]. As an irreversible pan-HER tyrosine kinase inhibitor, Pyrotinib exerts its antitumor effects by blocking the phosphorylation and activation of HER family receptors, including HER2 and epidermal growth factor receptor (EGFR). This upstream inhibition prevents activation of downstream signaling networks such as the PI3K/AKT axis. By reducing PI3K activity, Pyrotinib decreases AKT phosphorylation, thereby impairing survival and proliferative signaling. Concurrent suppression of the Rat sarcoma virus (RAS)/Rapidly accelerated fibrosarcoma (RAF)/MAPK ERK-kinase (MEK)/ERK pathway further enhances its therapeutic efficacy [21, 25, 26]. The findings of this study support the proposed dual-pathway inhibition mechanism of Pyrotinib and underscore its potential utility in targeting proliferative signaling in both oncologic and reproductive contexts.

Transcriptome sequencing revealed significant alterations in gene expression profiles following Pyrotinib treatment, with a notable enrichment of downregulated genes involved in chromatin remodeling and mitotic processes, including mitotic spindle assembly and chromosome segregation. These transcriptomic findings are consistent with cell cycle analysis results and further support the hypothesis that Pyrotinib may exert its antiproliferative effects on TM3 cells through multiple molecular pathways.

While this study provides preliminary insights into the potential reproductive toxicity of Pyrotinib in male subjects, several limitations should be acknowledged and addressed in future research. Although the TM3 mouse Leydig cell line serves as a useful model for studying aspects of male reproductive function [27–29], biological differences between rodent and human reproductive cells may limit the direct generalizability of the findings. Future studies incorporating human testicular cells or *in vivo* animal models are warranted to improve translational relevance. Moreover, the present investigation is confined to *in vitro* experiments and lacks corroborative clinical data. To comprehensively assess the safety and long-term reproductive impact of Pyrotinib in male patients, well-designed clinical studies are needed. Such efforts will be critical for establishing evidence-based guidelines for Pyrotinib use in male cancer patients and for optimizing treatment strategies to minimize adverse effects while preserving fertility and quality of life.

5. Conclusions

In summary, this study reveals the potential cytotoxic effects of Pyrotinib on male reproductive system cells and provides mechanistic insights into its impact on cell proliferation, apoptosis and signaling pathways. Given the expanding clinical use of Pyrotinib in the treatment of various malignancies, these findings offer important foundational data for evaluating its safety profile in male patients. Moreover, the results contribute to the optimization of clinical treatment strategies and may inform the development and application of related targeted therapies in the future. For young male patients or those concerned with fertility preservation, it is prudent to consider preventive measures-such as sperm cryopreservation-prior to initiating Pyrotinib therapy, in order to safeguard reproductive function.

AVAILABILITY OF DATA AND MATERIALS

RNA-seq data reported in this paper are deposited into the NCBI Gene Expression Omnibus database. The accession number is GSE291353.

AUTHOR CONTRIBUTIONS

XH—designed the research study. XH, ZJP, PZ and ZPX—performed the research. XH, ZJP, JT, HMT and JPH—analyzed the data. XH and ZJP—wrote the manuscript. JY—performed the bioinformatic analysis. All authors contributed to editorial changes in the manuscript. All authors read and approved the final manuscript.

ETHICS APPROVAL AND CONSENT TO PARTICIPATE

Not applicable.

ACKNOWLEDGMENT

Not applicable.

FUNDING

This research received no external funding.

CONFLICT OF INTEREST

The authors declare no conflict of interest.

SUPPLEMENTARY MATERIAL

Supplementary material associated with this article can be found, in the online version, at https://oss.jomh.org/

files/article/1950444709699567616/attachment/Supplementary%20material.docx.

REFERENCES

[1] Ziegengeist JL, Tan AR. A clinical review of subcutaneous trastuzumab and the fixed-dose combination of pertuzumab and trastuzumab for subcutaneous injection in the treatment of HER2-positive breast cancer. Clinical Breast Cancer. 2025; 25: e124–e132.

[2] Stanowicka-Grada M, Senkus E. Anti-HER2 drugs for the treatment of advanced HER2 positive breast cancer. Current Treatment Options in Oncology. 2023; 24: 1633–1650.

[3] Qi X, Shi Q, Xuhong J, Zhang Y, Jiang J. Pyrotinib-based therapeutic approaches for HER2-positive breast cancer: the time is now. Breast Cancer Research. 2023; 25: 113.

[4] Ma F, Li Q, Chen S, Zhu W, Fan Y, Wang J, *et al*. Phase I study and biomarker analysis of pyrotinib, a novel irreversible pan-ErbB receptor tyrosine kinase inhibitor, in patients with human epidermal growth factor receptor 2-positive metastatic breast cancer. Journal of Clinical Oncology. 2017; 35: 3105–3112.

[5] Li X, Yang C, Wan H, Zhang G, Feng J, Zhang L, *et al*. Discovery and development of pyrotinib: a novel irreversible EGFR/HER2 dual tyrosine kinase inhibitor with favorable safety profiles for the treatment of breast cancer. European Journal of Pharmaceutical Sciences. 2017; 110: 51–61.

[6] Zhang Q, He P, Tian T, Yan X, Huang J, Zhang Z, *et al*. Real-world efficacy and safety of pyrotinib in patients with HER2-positive metastatic breast cancer: a prospective real-world study. Frontiers in Pharmacology. 2023; 14: 1100556.

[7] Liu SM, Tu HY, Wei XW, Yan HH, Dong XR, Cui JW, *et al.* First-line pyrotinib in advanced HER2-mutant non-small-cell lung cancer: a patient-centric phase 2 trial. Nature Medicine. 2023; 29: 2079–2086.

[8] Liu D, Kou F, Gong J, Wang Z, Zhang X, Li J, *et al.* Pyrotinib alone or in combination with docetaxel in refractory HER2-positive gastric cancer: a dose-escalation phase I study. Cancer Medicine. 2023; 12: 10704–10714.

[9] Chen S, Zhou Y, Chen Y, Gu J. Fastp: an ultra-fast all-in-one FASTQ preprocessor. Bioinformatics. 2018; 34: i884–i890.

[10] Kim D, Langmead B, Salzberg SL. HISAT: a fast spliced aligner with low memory requirements. Nature Methods. 2015; 12: 357–360.

[11] Liao Y, Smyth GK, Shi W. FeatureCounts: an efficient general purpose program for assigning sequence reads to genomic features. Bioinformatics. 2014; 30: 923–930.

[12] Lê S, Josse J, Husson F. FactoMineR: an R package for multivariate analysis. Journal of Statistical Software. 2008; 25: 1–18.

[13] Love MI, Huber W, Anders S. Moderated estimation of fold change and dispersion for RNA-seq data with DESeq2. Genome Biology. 2014; 15: 550.

[14] Young MD, Wakefield MJ, Smyth GK, Oshlack A. Gene ontology analysis for RNA-seq: accounting for selection bias. Genome Biology. 2010; 11: R14.

[15] Kanehisa M, Goto S. KEGG: Kyoto encyclopedia of genes and genomes. Nucleic Acids Research. 2000; 28: 27–30.

[16] Yu G, Wang LG, Han Y, He QY. ClusterProfiler: an R package for comparing biological themes among gene clusters. OMICS: A Journal of Integrative Biology. 2012; 16: 284–287.

[17] Song Z, Lv D, Chen SQ, Huang J, Li Y, Ying S, *et al*. Pyrotinib in patients with HER2-amplified advanced non-small cell lung cancer: a prospective, multicenter, single-arm trial. Clinical Cancer Research. 2022; 28: 461–467.

[18] Wang L, Wu Y, Ren Z, Chu X, Chen J, Liu L, *et al.* A retrospective study of first-line therapy and subsequent pyrotinib treatment in advanced lung adenocarcinoma with HER2 mutations. Cancer Medicine. 2024; 13: e7335.

[19] Meng J, Liu XY, Ma S, Zhang H, Yu SD, Zhang YF, *et al*. Metabolism and disposition of pyrotinib in healthy male volunteers: covalent binding with human plasma protein. Acta Pharmacologica Sinica. 2019; 40: 980–988.

[20] Zirkin BR, Papadopoulos V. Leydig cells: formation, function, and regulation. Biology of Reproduction. 2018; 99: 101–111.

[21] Zhou L, Le K, Chen Q, Wang H. The efficacy and potential mechanisms of pyrotinib in targeting EGFR and HER2 in advanced oral squamous cell carcinoma. BMC Oral Health. 2024; 24: 898.

[22] Wu L, Huang S, Tian W, Liu P, Xie Y, Qiu Y, *et al.* PIWI-interacting RNA-YBX1 inhibits proliferation and metastasis by the MAPK signaling pathway via YBX1 in triple-negative breast cancer. Cell Death Discovery. 2024; 10: 7.

[23] Ou X, Tan Y, Xie J, Yuan J, Deng X, Shao R, *et al*. Methylation of GPRC5A promotes liver metastasis and docetaxel resistance through activating mTOR signaling pathway in triple negative breast cancer. Drug Resistance Updates. 2024; 73: 101063.

[24] Zhang HP, Jiang RY, Zhu JY, Sun KN, Huang Y, Zhou HH, *et al*. PI3K/AKT/mTOR signaling pathway: an important driver and therapeutic target in triple-negative breast cancer. Breast Cancer. 2024; 31: 539–551.

[25] Zhang K, Hong R, Kaping L, Xu F, Xia W, Qin G, *et al*. CDK4/6 inhibitor palbociclib enhances the effect of pyrotinib in HER2-positive breast cancer. Cancer Letters. 2019; 447: 130–140.

[26] Chen H, Si Y, Wen J, Hu C, Xia E, Wang Y, *et al*. P110alpha inhibitor alpelisib exhibits a synergistic effect with pyrotinib and reverses pyrotinib resistant in HER2+ breast cancer. Neoplasia. 2023; 43: 100913.

[27] Orta-Yilmaz B, Korkut A, Aydin Y. The impact of furan exposure on steroidogenesis in Leydig cells: cellular and molecular observations. Molecular Biology Reports. 2024; 51: 1047.

[28] Leisegang K, Henkel R. The *in vitro* modulation of steroidogenesis by inflammatory cytokines and insulin in TM3 Leydig cells. Reproductive Biology and Endocrinology. 2018; 16: 26.

[29] Tian M, Cao H, Gao H, Zhu L, Wu Y, Li G. Rotenone-induced cell apoptosis via endoplasmic reticulum stress and PERK-eIF2alpha-CHOP signalling pathways in TM3 cells. Ecotoxicology and Environmental Safety. 2024; 284: 116972.

How to cite this article: Xiao Hu, Zhongjian Pan, Jie Yang, Peng Zheng, Jian Tan, Zhipeng Xu, *et al*. The toxicity and mechanisms of pyrotinib on male reproductive system. Journal of Men's Health. 2025; 21(7): 107-114. doi: 10.22514/jomh.2025.102.